Journal of Sound and Vibration (1997) **206**(3), 399–423

VIBRATION ANALYSIS AND SUPPRESSION CONTROL OF AN ELEVATOR STRING ACTUATED BY A PM SYNCHRONOUS SERVO MOTOR

R.-F. FUNG AND J.-H. LIN

Department of Mechanical Engineering, Chung Yuan Christian University, Chung-Li, Taiwan 32023, *Republic of China*

AND

C.-M. YAO

National Center for High-Performance Computing, Hsinchu, Taiwan, Republic of China

(*Received* 6 *November* 1996, *and in final form* 23 *April* 1997)

This paper presents the vibration analysis and suppression control of a moving elevator string. A dynamic formulation is proposed first for the non-linear vibrations of the string with time-varying length and a weight attached at the lower end. The permanent magnet (PM) synchronous servo motor is used as the actuator to drive the rotor. A set of non-linear, time-varying differential equations describing this system is derived by Hamilton's principle. Due to the winding of the string either on or off the rotor, the mass and inertia of the rotor are time-dependent. The Galerkin method is used with time-dependent basis functions to determine the approximate solutions. A variable structure control (VSC) scheme is applied to suppress the transient amplitudes of vibrations. The sliding surfaces are determined in terms of the errors between the system states and the ideal states of the string and the rotor. The numerical results show that the motion-induced vibrations of the moving string and the tracking performance of the rotor can be controlled effectively.

1. INTRODUCTION

The system is composed of a string with time-varying length [1, 2] and a mass attached at the lower end is considered to be a basic model of an elevator in a building. For the problem of string vibrations with time-varying length, Kotera and Kawai [3] analyzed free vibration by the Laplace transformation. Fung and Cheng [4] studied the free vibration of a string/slider system with non-linear coupling. As far as the string vibration is concerned, little work has appeared on the coupled oscillation, both from the point of view of the theoretical formulation of the problem and the analysis of the structural behavior. Moreover, the problem involving the oscillations of a textile machine rotor on which the textile is wound up was presented in a series of papers by Cventicanin [5, 6]. The dynamics of a rotor with variable mass are given by Bessonov [7]. Usually, the rotor consists of a disk which is symmetrically mounted at the middle of the shaft. The mass of the rotor is varying due to winding on or off the band.

In recent years advancements in magnetic materials, semiconductor power devices, and control theory have made the PM synchronous servo motor play a vitally important role in the motion-control applications in the low-to-medium power range. The desirable

0022–460X/97/380399 + 25 $25.00/0/sv971102

features of the PM synchronous servo motor are its compact structure, high airgap flux density, high power density, high torque-to-inertia ratio, and high torque capability. Moreover, compared with an induction servo motor, a PM synchronous servo motor has such advantages as higher efficiency, due to the absence of rotor losses and lower no-load current below the rated speed, with its decoupling control performance being much less sensitive to the parameter variations of the motor [8, 9]. To achieve fast four-quadrant operation and smooth starting and acceleration, the field-oriented control [10], or vector control, is used in the design of the PM synchronous servo motor drive.

Vibration of the moving continua usually limits their utility in many applications, and particularly in high speed, precision systems. Vibration control is an important approach to improve performance in these systems. Previously, vibration reduction is generally achieved through the modifications in design to increase the effective stiffness or damping. In addition, active vibration control has been receiving increasing interest in recent years [11]. The active control, in general, requires continuous monitoring of the responses [12]. Radcliffe and Mote [13] developed a laboratory active control system for circular saws where electromagnets were used to increase the effective damping and stiffness of transverse vibrations. Mote and Holoyen [14] also developed an active control system for temperature control of a circular saw. Controlling saw temperature is one indirect method which reduces saw vibration through effective stiffness modification.

A moving string belongs to a class of distributed parameter systems. Control of distributed parameter systems is gradually being noticed [15, 16]. Ulsoy [17] studied the active vibration problem through pole allocation and used an adaptive control scheme which takes into account the vibration induced by the translation motion of the string. From a practical point of view, Yang and Mote [18] presented a method for active vibration control of an axially moving string. They accounted for the dynamics of actuators and sensors. The control was formulated in the Laplace transform domain and carried out by analyzing the root loci of the closed-loop system.

The use of the sliding mode technique, derived from the variable structure control (VSC) theory, has been widely considered for both linear and non-linear systems [19]. A general VSC design method has been developed and the property of well robustness of a VSC system with respect to system perturbation and disturbance has now been recognized [20–22]. In fact, VSC has been applied to some flexible structures. Ficola *et al*. [23] presented a simplified strategy to implement VSC of a robot with a flexible forearm. Fung and Liao [24] studied the vibration reduction in an axially moving string by the application of a VSC scheme. The design of the VSC controller is based on the independent mode space control (IMSC) method. The major aspect in VSC theory is implemented by the sliding mode. The design of the controller consists of enforcing the system motion on some manifold in system state space.

In this paper, the coupled dynamic equations for the elevator system are derived by Hamilton's principle. The rotating rotor with variable mass and inertia is considered. In addition, the coupling provides the opportunity that the transverse vibration of the string can be suppressed by the control acting on the current of the PM synchronous servo motor. The organization of the paper is as follows. In section 2, the coupled model for the elevator system including both the motions of the string and the rotor are described and formulated. In section 3, the non-dimensional variables are defined and the Galerkin method used with a time-dependent basis function, to determine the approximate solutions. In section 4, a general matrix form of the equations of motion for the elevator system is formulated. Then, design of the VSC controller is discussed. In section 5, numerical results include: (i) vibration responses of the elevator system presented to deal with the motion-induced vibration and convergence analysis of the transient responses of the coupled system; (ii)

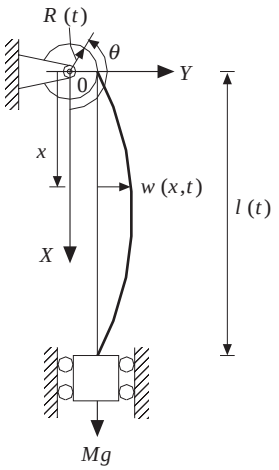

Figure 1. The sketch of the elevator system.

implementation of vibration suppression based on the VSC algorithm. Finally, the conclusions are drawn in section 6.

2. EQUATIONS OF MOTION

2.1. GEOMETRY DESCRIPTION

In Figure 1, the elevator system is shown and a plane Cartesian co-ordinate system is adopted. The rotation of rotor is driven by a PM synchronous servo motor. Figure 2 shows the PM synchronous servo motor including a geared speed-reducer. The mass per unit length of the string is ρ, and its transport velocity is $\dot{x}$ and acceleration is $\ddot{x}$. The length of the string at time t is $l(t)$, and the radius of the rotor at time t is $R(t)$. Neglecting the effect of sag, the cable is considered as a linear elastic string. The string is wound on a drum at the top end and a mass M is attached at its lower end. The mass is allowed to move along the x direction only. The transverse displacement of the string at an axial position x is described by the field variable $w(x, t)$. The string is subjected to an initial tension T which is due to the weight of the attached mass and the string weight and is assumed to be simply supported at $x = 0$ and $l(t)$ due to small vibration assumption.

Since the connection point $(0, R(t))$ is common to the rotor and string, this point on the string has the same velocity and acceleration as that on the rotor in the tangential direction.

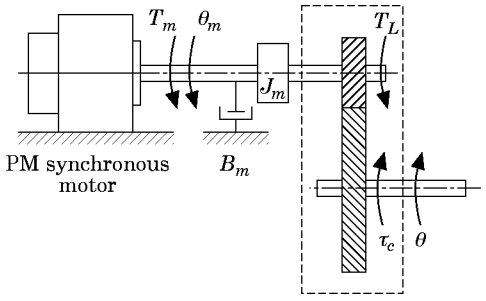

Figure 2. Schematic of the motor-gear mechanism.

2.2. VIBRATION STRING

The function of the rotor is to wind the string on or off, so that the rotor mass is variable. In Figure 1, $R(t)$ is the radius of the disk, and θ is the rotary angle. The string is subjected to an initial tension $T(x, l(t))$ which is represented by equation (A4) of Appendix A, so this force acts along the tangent line of the rotor in the undeformed configuration. From the geometry of Figure 1, the time-varying length of the string is given by

$$l(t) = l_0 - \int_0^\theta R(\varepsilon)\,\mathrm{d}\varepsilon, \tag{1}$$

where l_0 is the string length at initial time and R is a function of θ which is described in equation (3).

2.3. ROTATING ROTOR

The rotor is modelled as a rigid disk mounted on a massless shaft which is supported by two perfect rotating bearings. As given in the papers by Cventianin [5] and Tsai [25], the time-varying mass $m(t)$ and radius $R(t)$ of the rotor are assumed to be

$$m(t) = m_0 + R_1\rho\theta(t), \qquad R(t) = (R_0^2 + R_1 h\theta(t)/\pi)^{1/2} \tag{2, 3}$$

respectively, where m_0 and R_0 are the initial mass and initial radius of the rotor, respectively, $\theta(t)$ is the angular velocity of the rotor and has a positive value for the string to be wound on, $R_1 = R_0 + h/2$, and h is the average thickness of the string.

The governing equations can be written as (the derivations are detailed in Appendix A)

$$w_{tt} + 2\dot{x}w_{xt} + (\ddot{x} + g)w_x - [\dot{x}^2 - Mg/\rho - g(l(t) - x)]w_{xx} - \tfrac{3}{2}(EA/\rho)w_x^2 w_{xx} = -\ddot{R}(t), \quad 0 < x < l(t) \tag{4a}$$

$$\ddot{\theta} + [\dot{I}(t)/I(t)]\dot{\theta} + [R(t)/2I(t)]\{\rho[\dot{x}^2 + \dot{x}^2 w_x^2(l(t), t) + \dot{R}^2(t) + 2\dot{x}\dot{R}w_x(l(t), t)] - [Mgw_x^2(l(t), t) + \tfrac{1}{4}EAw_x^4(l(t), t)] + 2Mg + 2\rho g l(t)\} = \tau_e/I(t), \tag{4b}$$

and the boundary conditions are

$$w(0, t) = 0, \qquad w(l(t), t) = 0. \tag{5a, 5b}$$

where τ_e is the torque applied to the rotor, $I(t) = \frac{1}{2}m(t)R^2(t)$ is the inertia of the rotor and

$$\dot{x} = -R(t)\dot{\theta}, \qquad \ddot{x} = -\dot{R}(t)\dot{\theta} - R(t)\ddot{\theta}. \tag{6a, 6b}$$

Some remarks are made here:

(i) In this paper, the longitudinal elastic deformation of the string is neglected, so every point along the string has the same axial travelling velocity $\dot{x}$ and acceleration $\ddot{x}$, which are given by equations (6a, 6b).

(ii) The terms containing EA in equations (4a, 4b) are due to the geometric non-linearity of the string. If they are neglected for the small-amplitude transverse vibrations of the string, the governing equation (4a) becomes linear. However, equation (4b) is still non-linear, due to the coupling at the boundary $x = l(t)$.

(iii) For the case with constant angular velocity, the radius $R(t)$ of the rotor and the axial velocity $\dot{x}$ of the string are still functions of time. Thus, $\dot{R}(t)$ is not equal to zero, and the axial travelling acceleration $\ddot{x}$ also exists.

(iv) The terms including $w_x(l(t), t)$ in equation (4b) are the end effect at $x = l(t)$ of the string vibration on the rotor.

(v) The mass and inertia of the rotor are time-varying when the string is wound on or off, therefore the non-linear governing equations (4a, 4b) include the time-dependent mass $m(t)$ and inertia $I(t)$.

2.4. PM SYNCHRONOUS SERVO MOTOR DRIVE

The machine model of a PM synchronous motor can be described in the rotor rotating reference frame as follows [9, 10].

$$v_q = R_s i_q + p\lambda_q + \omega_s \lambda_d, \qquad v_d = R_s i_d + p\lambda_d - \omega_s \lambda_q, \tag{7, 8}$$

where p denotes the differential operator d/dt and

$$\lambda_q = L_q i_q, \qquad \lambda_d = L_d i_d + L_{md} I_{fd}. \tag{9, 10}$$

In the above equations v_d and v_q are the d, q axis stator voltages, i_d and i_q are the d, q axis stator currents, L_d and L_q are the d, q axis inductances, λ_d and λ_q are the d, q axis stator flux linkages, while R_s and ω_s are the stator resistance and inverter frequency, respectively. In equation (10) I_{fd} is the equivalent d-axis magnetizing current, and L_{md} is the d-axis mutual inductance.

The electric torque

$$T_L = (3P/2)[L_{md} I_{fd} i_q + (L_d - L_q) i_d i_q], \tag{11}$$

and the equation for the motor dynamics is

$$T_m = T_L + B_m \dot{\theta}_m + J_m p \dot{\theta}_m. \tag{12}$$

In equation (11), P is the number of pole pairs, T_L is the electric torque, B_m is the damping coefficient, $\dot{\theta}_m$ is the rotor speed and J_m is the moment of inertia of rotor in the PM motor.

The basic principle in controlling a PM synchronous motor drive is based on the field orientation. The configuration of a general field-oriented PM synchronous motor drive

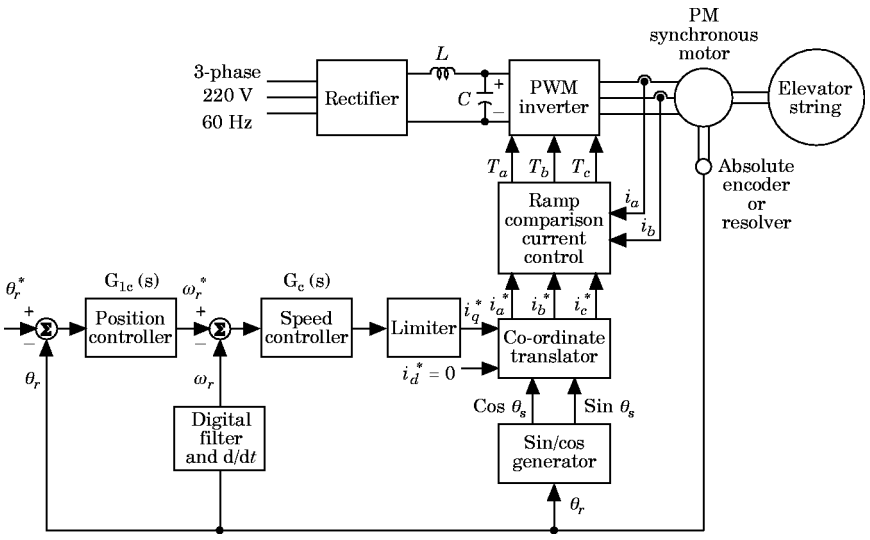

Figure 3. The field-oriented PM synchronous servo motor drive system.

system is shown in Figure 3. With the implementation of field-oriented control, some relationships are proposed [9] in the PM synchronous motor drive system as follows

$$T_m = K_T i_q, \qquad K_T = \tfrac{3}{2} P L_{md} I_{fd}, \tag{13, 14}$$

From Figure 2, a PM synchronous motor system includes a geared speed reducer with a gear ratio

$$r = T_L/\tau_e = \dot{\theta}/\dot{\theta}_m. \tag{15}$$

Using equations (15) and (12), the following applied torque can be obtained

$$r\tau_e = T_L = T_m - J_m\ddot{\theta}_m - B_m\dot{\theta}_m. \tag{16}$$

2.5. GOVERNING EQUATIONS OF THE ELEVATOR-PLUS-ACTUATOR SYSTEM

With implementation of the field-oriented control, the PM synchronous motor drive can be simplified to a control system. Now one substitutes equations (13) and (16) into equation (4b) to obtain

$$J_m\ddot{\theta}_m + B_m\dot{\theta}_m + r\{I(t)\ddot{\theta}(t) + \dot{I}(t)\dot{\theta}(t) + (R(t)/2)[\dot{x}^2 + \dot{x}^2 w_x(l(t), t) + \dot{R}^2(t) + 2\dot{x}\dot{R}w_x(l(t), t) - Mgw_x^2(l(t), t) - \tfrac{1}{4}EAw_x^4(l(t), t) + 2g(M + \rho l(t))\} = K_T i_q. \tag{17}$$

From the relationship between θ and θ_m in equation (15), equation (17) is formulated as

$$\ddot{\theta} + \frac{B_m + r^2\dot{I}(t)}{J_m + r^2 I(t)}\dot{\theta} + \frac{r^2 R(t)}{2(J_m + r^2 I(t))}\{\rho[\dot{x}^2 + \dot{x}^2 w_x^2(l(t), t) + \dot{R}^2(t) + 2\dot{x}\dot{R}w_x(l(t), t) - Mgw_x^2(l(t), t) - \tfrac{1}{4}EAw_x^4(l(t), t) + 2Mg + 2\rho g l(t)\} = \frac{rK_T i_q}{J_m + r^2 I(t)}. \tag{18}$$

Equation (4a) and equation (18) constitute the governing equations of the elevator-plus-actuator system.

3. METHOD OF SOLUTION

3.1. DIMENSIONLESS FORM OF THE GOVERNING EQUATIONS

For convenience in determining the influence of the parameters of the coupled system, one defines the following non-dimensional variables and parameters:

$$W = w/l_0, \quad \xi = x/l_0, \quad \tau = c_2 t/l_0, \quad \overline{l} = l(t)/l_0, \quad \bar{g} = gl_0/c_2^2, \quad \Lambda_m = J_m/\rho l_0^3,$$
$$\overline{B}_M = B_m/\rho c_2 l_0^2, \quad \overline{R} = R(t)/l_0, \quad \overline{I} = I(t)/\rho l_0^3, \quad \overline{M} = M/\rho l_0,$$
$$\overline{A}_Q = K_T i_q/\rho c_2^2 l_0, \quad \beta = c_1/c_2, \tag{19}$$

where $c_1 = \sqrt{EA/\rho}$, $c_2 = \sqrt{T_0/\rho}$, which are the wave velocities of the string in the longitudinal and transverse directions, respectively. Then equation (4a) and equation (18) in non-dimensional form are

$$W_{\tau\tau} + 2\xi_\tau W_{\xi\tau} + (\xi_{\tau\tau} + g)W_\xi + [\xi_\tau^2 - 1 - (1/\overline{M})(\overline{l} - \xi)]W_{\xi\xi} - \tfrac{3}{2}\beta^2 W_\xi^2 W_{\xi\xi} = -\overline{R}_{\tau\tau}, \quad 0 < \xi < \overline{l}, \tag{20a}$$

$$\theta_{\tau\tau} + \frac{\bar{B}_M + r^2\bar{I}_\tau}{\Lambda_M + r^2\bar{I}}\theta_\tau + \frac{r^2\bar{R}}{2(\Lambda_M + r^2\bar{I})}\{[\xi_\tau^2 + \bar{R}_\tau^2 + 2\xi_\tau\bar{R}_\tau W_\xi(\bar{l},\tau) + \xi_\tau^2 W_\xi^2(\bar{l},\tau)]$$
$$- [\bar{M}\bar{g}W_\xi^2(\bar{l},\tau) + \tfrac{1}{4}\beta^2 W_\xi^4(\bar{l},\tau)] + 2\bar{g}(\bar{M} + \bar{l}\} = r\bar{A}_Q/(\Lambda_M + r^2\bar{I}), \qquad (20b)$$

and the non-dimensional boundary conditions are

$$W(0,\tau) = 0, \qquad W(\bar{l},\tau) = 0. \qquad (21a, 21b)$$

3.2. APPROXIMATE SOLUTION BY THE GALERKIN METHOD

The spatial dependence can be eliminated from the equations of the coupled system to yield a set of ordinary differential equations in time, which can be solved for the system response. The approximate solution derived in this section is based on a Galerkin approximation with time-dependent basis functions. This technique was used by Fung and Cheng [4] to investigate the free vibration of a non-linear coupled string/slider system with a moving boundary. Based on this method, the forms of the displacements are assumed to satisfy the geometric boundary conditions of the string, that is

$$W(\xi,\tau) = \sum_{n=1}^{\infty}\varphi_n(\xi,\bar{l})q_n(\tau), \qquad 0 < \xi < \bar{l}, \qquad (22)$$

where $q_n(\tau)$ are the generalized co-ordinates and the shape functions of the space variable are

$$\varphi_n(\xi,\bar{l}) = \alpha_n(\tau)\sin[\Omega_n(\tau)\xi], \qquad n = 1, 2, 3\ldots, \qquad (23)$$

in which

$$\Omega_n(\tau) = n\pi/\bar{l}, \qquad \alpha_n(\tau) = \sqrt{2/\bar{l}}, \qquad n = 1, 2, 3\ldots. \qquad (24)$$

α_n is used to normalize the shape function. Since the spatial domain is time-dependent, both eigenfunctions $\varphi_n(\xi,\bar{l})$ and eigenvalues $\Omega_n(\tau)$ are time-dependent.

Substituting equations (22), (23) and (24) into (20a) and (20b), taking inner products and making use of the orthogonality property, one has a set of non-linear time-varying ordinary differential equations

$$\ddot{q}_m + \sum_{n=1}^{\infty}[a_{mn}(\bar{l},\dot{\bar{l}})\dot{q}_n + b_{mn}(\bar{l},\dot{\bar{l}},\ddot{\bar{l}})q_n] - \sum_{i=1}^{\infty}\sum_{j=1}^{\infty}\sum_{k=1}^{\infty}c_{mijk}(\bar{l})q_i q_j q_k = G_m, \qquad (25a)$$

$$\ddot{\theta} + a^r\dot{\theta} + \sum_{n=1}^{\infty}b_n^r(\bar{l})q_n + \sum_{n=1}^{\infty}\sum_{i=1}^{\infty}c_{ni}^r(\bar{l})q_n q_i + \sum_{n=1}^{\infty}\sum_{i=1}^{\infty}\sum_{j=1}^{\infty}\sum_{k=1}^{\infty}d_{nijk}^r(\bar{l})q_n q_i q_j q_k = F^r(\bar{l}), \qquad (25b)$$

where $m, n, i, j, k = 1, 2, \ldots$ are the modes considered in the string system and all of the coefficients are presented in detail in Appendix B. In equations (25a) and (25b), the dot symbol is also used to represent the time derivative with respect to the non-dimensional time τ for a non-dimensional variable.

4. VARIABLE STRUCTURE CONTROL

4.1. SYSTEM DESCRIPTION IN THE STATE SPACE FORM

In this section, VSC algorithm is proposed to suppress the transient amplitudes of the

string vibrations. One rewrites the above non-linear coupled ordinary differential equations (25a) and (25b) in matrix form as

$$\mathbf{M}(\mathbf{X})\ddot{\mathbf{X}} + \mathbf{H}(\mathbf{X}, \dot{\mathbf{X}}) + \mathbf{K}(\mathbf{X})\mathbf{X} = \mathbf{U}, \tag{26}$$

where $\mathbf{M}(\mathbf{X}) \in R^{(N+1)(N+1)}$ is an inertia matrix, $\mathbf{X} = [q_1, q_2, q_3, \ldots, q_N, \theta]$ is the vector of variables, q_i are the unknown generalized co-ordinates in the Garlerkin discretization, $\mathbf{H}(\mathbf{X}, \dot{\mathbf{X}}) \in R^{N+1}$ is the vector of non-linear terms, $\mathbf{K}(\mathbf{X}) \in R^{(N+1)(N+1)}$ is a stiffness matrix and $\mathbf{U} \in R^{N+1}$ is the vector of the external input current which is supplied by the PM synchronous servo motor. N is the number of modes chosen for analysis. The details of matrix $\mathbf{M}(\mathbf{X})$, $\mathbf{H}(\mathbf{X}, \dot{\mathbf{X}})$, $\mathbf{K}(\mathbf{X})$ and $\mathbf{U}$ are shown in Appendix B.

By defining the state vector for the system as

$$\mathbf{x}(\tau) = [\mathbf{X}, \dot{\mathbf{X}}]^{\mathrm{T}} = [q_1, q_2, q_3, \ldots, q_N, \theta, \dot{q}_1, \dot{q}_2, \dot{q}_3, \ldots, \dot{q}_N, \dot{\theta}]^{\mathrm{T}}.$$

The dynamic equation in equation (26) can be rewritten in the state space:

$$\dot{\mathbf{x}}(\tau) = \mathbf{L}(\mathbf{x})\mathbf{x} + \mathbf{J}(\mathbf{x})u + \mathbf{N}(\mathbf{x}), \tag{27}$$

where $u = \bar{A}_Q$ is the control input of the state equation, and

$$\mathbf{L}(\mathbf{x}) = \begin{bmatrix} [\mathbf{0}]_{(N+1)(N+1)} & \mathbf{I} \\ -\mathbf{M}^{-1}\mathbf{K} & [\mathbf{0}]_{(N+1)(N+1)} \end{bmatrix}, \qquad \mathbf{J}(\mathbf{x}) = \begin{bmatrix} [\mathbf{0}]_{N+1} \\ \mathbf{M}^{-1}\mathbf{B}' \end{bmatrix},$$

$$\mathbf{N}(\mathbf{x}) = \begin{bmatrix} [\mathbf{0}]_{N+1} \\ -\mathbf{M}^{-1}\mathbf{H} \end{bmatrix}, \qquad \mathbf{B}' = \begin{bmatrix} [\mathbf{0}]_{N+1} \\ 1 \end{bmatrix}.$$

Suppose that the desired state $\mathbf{x}_d(\tau) = [x_{1d}, x_{2d}, x_{3d}, \ldots, x_{(2N+2)d}]^{\mathrm{T}}$ has been selected for the desired behavior of the state variables. A choice is given by

$$x_{1d} = q_{1d} = 0, \qquad x_{2d} = q_{2d} = 0, \ldots, x_{Nd} = q_{Nd} = 0, \qquad x_{(N+1)d} = \theta_d,$$

$$x_{(N+2)d} = \dot{q}_{1d} = 0, \qquad x_{(N+3)d} = \dot{q}_{2d} = 0, \ldots, x_{(2N+1)d} = \dot{q}_{Nd} = 0, \qquad x_{(2N+2)d} = \dot{\theta}_d.$$

Physically, they represent zero transverse deflection during the desired motion of rotor. To ensure trajectory tracking in VSC law by the state variables, one defines the tracking errors as

$$\mathbf{e} = [e_i, e_2, e_3, \ldots, e_{2N+2}]^{\mathrm{T}} = \mathbf{x}(\tau) - \mathbf{x}_d(\tau). \tag{28}$$

Then the following switching surface $S \in R$ is defined as a hypersurface

$$S(\mathbf{e}) = \mathbf{C}\mathbf{e}, \tag{29}$$

where $\mathbf{C} = [c_1, c_2, c_3, \ldots, c_{2N+2}]$, c_i are constants. Also S can be written in the specific form:

$$S = \sum_{i=1}^{2N+2} c_i e_i. \tag{30}$$

4.2. REACHING LAW METHOD OF THE VSC ALGORITHM

The main requirement in the reaching mode design is that the control should satisfy the reaching condition, which in turn guarantees the existence of the sliding mode on the switching manifold. Additional requirements include fast reaching and low chattering.

Specifying a scheme for the switching order is also a part of a VSC design. In this subsection, the reaching law method is introduced.

The reaching law is one differential equation which specifies the dynamics of a switching function. The differential equation of an asymptotically stable switching function is itself a reaching condition. In addition, by the choice of the parameters in the differential equation, the dynamic quality of VSC in the reaching mode can be controlled. The treatment given here is to define the reaching law as

$$\dot{S} = -PS - Q|S|^k(S/(|S| + \delta)), \qquad 0 < k < 1, \tag{31}$$

where P and Q are constant coefficients and δ is the boundary layer. The reaching law increases the reaching time and speed when the state is far away from the switching manifold. In particular, the reaching law can reduce the hitting time in the reaching phase by a choice in [26]. Moreover, the reaching law in [24] increases the reaching speed when the state is far away from the switching manifold and reduces the rate when the state is nearby. Therefore, the state is enforced to approach the switching manifold fast by the choice of equation (31). The selecting of the reaching law guarantees the convergence of the trajectory to the sliding surface described by equation (30). It can be easily proved that

$$\dot{S}S < 0.$$

Differentiating S in equation (30) with respect to time gives the sliding mode equation

$$\dot{S} = \mathbf{C}\dot{\mathbf{e}} = \sum_{i=1}^{2N+2} c_i \dot{e}_i = \sum_{i=1}^{N+1} c_i e_{i+N+1} + \sum_{i=N+2}^{2N+1} c_i \left(\sum_{j=1}^{N} L_{ij} x_j + J_i u + n_i \right)$$

$$+ (L_{2N+2,j} x_j + J_{2N+2} u + n_{2N+2} - \ddot{\theta}_d). \tag{32}$$

From equations (31) and (32), one obtains the control input u,

$$u = \frac{1}{\Delta} \left[-PS - Q|S|^k \frac{S}{|S| + \delta} - \sum_{i=1}^{N+1} c_i e_{i+N+1} - \sum_{i=N+2}^{2N+1} c_i \left(\sum_{j=1}^{N} L_{ij} x_j + n_i \right) \right.$$

$$\left. - \left(\sum_{j=1}^{N} L_{2N+2,j} x_j + n_{2N+2} \right) + \ddot{\theta}_d \right], \tag{33}$$

where

$$\Delta = \sum_{i=N+2}^{2N+1} c_i J_i + J_{2N+2}.$$

5. NUMERICAL RESULTS AND DISCUSSION

During numerical simulations, the convergence of the transient responses of the Garlerkin method and the motion-induced vibration problems of the elevator system are proposed. The dynamic equations of the elevator system in equations (25a) and (25b) are integrated by the Runge–Kutta method. The examples given here are chosen to study the coupling effect on the transient vibrations of the elevator system. The parameters are $T_0 = 100$ N, $\rho = 1$ kg/m, $m_0 = 4{\cdot}95$ kg, $h = 0{\cdot}02$ m, $K_T = 0{\cdot}9$ Nm/A,

$J_m = 3{\cdot}92 \times 10^{-3}$ N m s^2 and $B_m = 1 \times 10^{-3}$ N m s/rad. Our purpose is to acquire fundamental knowledge about the transverse vibrations of the moving string with zero initial values $q_i(0) = 0$. In the governing equation (25a), the responses q_i depend on the non-homogeneous term G_m whose detailed expression is shown in Appendix C. It means that the variation of the rotor radius excites the transverse vibrations of the moving string. In addition, from the remark (i) stated in section 2, one can obtain the relationships $\dot{x} = \dot{l}$ and $\ddot{x} = \ddot{l}$. Thus, the variation of the rotor is also governed by the time history of the string motion. In the following section, some specific motions of the rotor and the string will be simulated where $q_i(0) = 0$, $\dot{q}_i(0) = 0$.

5.1. VIBRATION ANALYSIS

5.1.1. *Convergence analysis of the transient responses*

In this study, it is necessary to know whether or not the transient response converges as the number of terms in the Galerkin discretization increases. Usually, the norm of the generalized co-ordinates is used for the analysis. One defines

$$|F_m| = \left(\sum_{i=1}^{m} q_i^2 \right)^{1/2}, \qquad \Delta F_{m-1,m} = |F_m| - |F_{m-1}|, \tag{34, 35}$$

where m is the maximum mode number taken.

A Hermite polynomial is chosen as the desired time history of the dimensionless string length $\bar{l}_d(\tau)$. It is written as

$$\bar{l}_d(\tau) = \bar{l}_i + (\bar{l}_f - \bar{l}_i)\left(70\frac{\tau^9}{\tau_f^9} - 315\frac{\tau^8}{\tau_f^8} + 540\frac{\tau^7}{\tau_f^7} - 420\frac{\tau^6}{\tau_f^6} + 126\frac{\tau^5}{\tau_f^5} \right), \tag{36}$$

where τ_f is the dimensionless ending time, $\bar{l}_i$ is the initial string length and $\bar{l}_f$ is the final string length. Figures 4(a–d) show the difference of the norms evaluated by equation (34) and the parameters are $\tau_f = 2$, $\bar{l}_i = 1$ and $\bar{l}_f = 0{\cdot}2$ in equation (36). The number of modes is increased from 3 to 9. It is seen that the difference between eight- and nine-term approximations is reduced to a quite small value. For this reason, it is observed that the transient response converges when the number $m = 9$ is taken in the Garlerkin

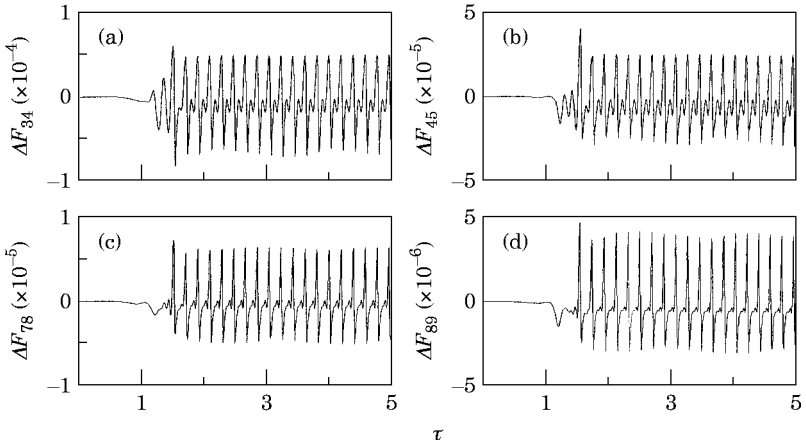

Figure 4. The difference between the norms of the generalized co-ordinates. (a) mode 4 minus mode 3, (b) mode 5 minus mode 4, (c) mode 8 minus mode 7, (d) mode 9 minus mode 8.

discretization. To save printing space, the vibration amplitudes of the first four modes ($m = 4$) are shown for discussing the vibration phenomena of a moving string.

5.1.2. *Motion-induced vibration*

Observing equation (25a), if the motion of the rotor is known or specified, i.e., $\bar{R}_{\tau\tau}$ is given, the time history of the transverse vibration of the string could be completely determined. The motion-induced vibration of the elevator system is governed by equation (25a), and can be obtained by directly integrating this equation. The reference input is selected to coincide with the entire motion of an elevator. In general, the operation of a motor includes three steps: accelerating from rest, maintaining a constant speed and decelerating to rest. Thus, the time history of the velocity follows a trapezoidal function while the motor is in running order. Moreover, we choose the other kinds of reference inputs which are smoother than the trapezoidal function to implement the motion-induced vibration and compare them. In this section, the trajectories of the angular position θ are given as the trapezoidal velocity, cycloidal and simple harmonic functions.

Case 1: trapezoidal function. In this section, the trapezoidal function of the angular velocity of the rotor is assigned. The desired angular velocity $\dot{\theta}_d$ versus the dimensionless time τ is given by

$$\pm\dot{\theta}_d = \begin{cases} \frac{40}{3}\pi/\tau & 0 \leqslant \tau \leqslant 0{\cdot}5 \\ \frac{20}{3}\pi & 0{\cdot}5 < \tau \leqslant 1{\cdot}5 \\ \frac{20}{3}\pi - \frac{40}{3}\pi\ (\tau - 1{\cdot}5) & 1{\cdot}5 < \tau \leqslant 2 \\ 0 & 2 < \tau \end{cases}. \tag{37}$$

The sign $\pm$ denotes the directions of the rotating rotor during winding on and off. $\dot{\theta}_d$ has a positive value when the string is being wound on. During retraction (extrusion), one takes the initial length of string $l_0 = 10$ m ($l_0 = 2$ m) and initial radius $R_0 = 0{\cdot}2$ m ($R_0 = 0{\cdot}26$ m). In Figures 5(a–h), the transient responses of the transverse vibrations for the first four modes during extrusion and retraction are compared. The solid line is used for the retraction while the dash line is used for the extrusion. In these figures, the vibration amplitudes q_1, q_2, q_3 and q_4 are excited simultaneously by the non-homogeneous term G_m. The time history θ having positive or negative values depends on whether the string is wound on or off. It is seen that the vibration amplitudes for the first four modes are gradually reduced and the frequencies increase when the string is wound on. Conversely, the vibration amplitudes increase gradually and the frequencies decrease when the string is wound off. Meanwhile, the residual vibrations of the first four modes occur after the ending time $\tau = 2$.

Case 2: cycloidal function. In this subsection, the cycloidal function is used as the trajectory of $\theta(\tau)$ to discuss the motion-induced vibration problem. The desired function $\theta_d(\tau)$ during retraction is written as

$$\theta_d(\tau) = \theta_i + (\theta_f - \theta_i)[\tau/\tau_f - (1/2\pi)\sin(2\pi\tau/\tau_f)], \tag{38}$$

where one chooses the end time $\tau_f = 2$, the initial angular position $\theta_i = 0$, and the final angular position is $\theta_f = 10\pi$ during retraction and $\theta_f = -10\pi$ during extrusion. These values are the same as those in case 1. In Figures 6(a–h), the transient responses of the moving string for the first four modes during extrusion and retraction are plotted. The solid line is used for the retraction while the dash line is used for the extrusion. It is shown that the vibration amplitudes gradually increase and the frequencies for the first four modes slow down when the length of the string increases. Correspondingly, the amplitudes of vibration decrease and the frequencies increase when the string length decreases. The

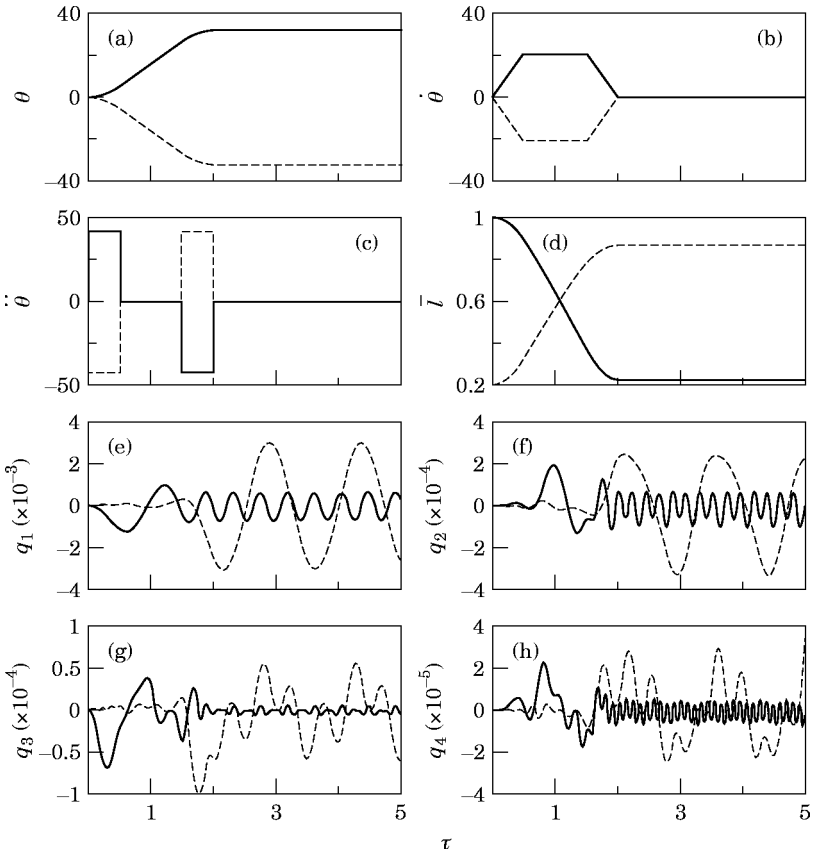

Figure 5. Motion-induced vibration with a desired trapezoidal function during extraction and retraction. (a) desired angular position, (b) desired angular velocity, (c) desired angular acceleration, (d) length of the string, (e) vibration amplitudes of mode 1, (f) vibration amplitudes of mode 2, (g) vibration amplitudes of mode 3, (h) vibration amplitudes of mode 4. (——, retraction; – – – –, extrusion.)

dominant vibrations of the elevator string occur when the extrusion motion is complete. In addition, the amplitude and frequency of the residual vibrations after $\tau_f = 2$ are constants as the motion is complete. These residual amplitudes will be suppressed by variable structure control.

At this point one considers the vibration results in cases 1 and 2. These transverse amplitudes are quite small due to the small values of the non-homogeneous terms. In fact, the variation of the rotor radius $R(t)$ is much slower than those of the angular position θ and the string length l. Although the angular velocities of the rotor shown in Figures 5(b) and 6(b) and the speeds of extrusion and retraction shown in Figures 5(d) and 6(d) are very fast, the variation of the rotor radius is still not apparent (not shown here).

Case 3: simple harmonic function. In case 3, the trajectory used in the motion-induced vibration is a simple harmonic function as follows.

$$\theta_d(\tau) = \theta_i + ((\theta_f - \theta_i)/2)(1 - \cos(\pi\tau/\tau_f)). \tag{39}$$

The values θ_i, θ_f and τ_f are the same as in case 2. The comparisons of the motion of the rotor and the transient responses of the string for cases 1, 2 and 3 are shown in

Figures 7(a–f). It can be observed that one obtains lower frequencies and smaller transient amplitudes for modes 1 and 2 as the simple harmonic motion is used.

Time histories of the string length and its transverse transient responses during retraction are shown in Figures 8(a–g). The response of the first four modes are shown for the comparison between the linear case ($\beta = 0$, solid line) and the non-linear one ($\beta = 10$, dash line). The Hermite polynomial is used as the desired motion of the string. It is observed that the frequencies of transient responses are higher when the non-linear term is considered. In addition, the influence of the non-linear term is gradually apparent during retraction and a beating phenomenon occurs after the ending time $\tau_f = 2$. When the motion of the string is complete, the non-linear term becomes very important. It is due to the fact that decreasing $\bar{l}(\tau)$ causes the increasing of the non-linear term. At the same time, a free vibration occurs after $\tau_f = 2$ and $q(2)$ and $\dot{q}(2)$ are the initial conditions for the free vibration of the string. Thus, the beating phenomenon is affected by the scale of the non-linear term at $\bar{l}_f = 0{\cdot}2$ and the initial conditions.

5.2. VIBRATION SUPPRESSION CONTROL

It has been discussed previously that the desired motion of rotor excites the transverse vibrations of the string. The string has residual oscillations after the motion is complete.

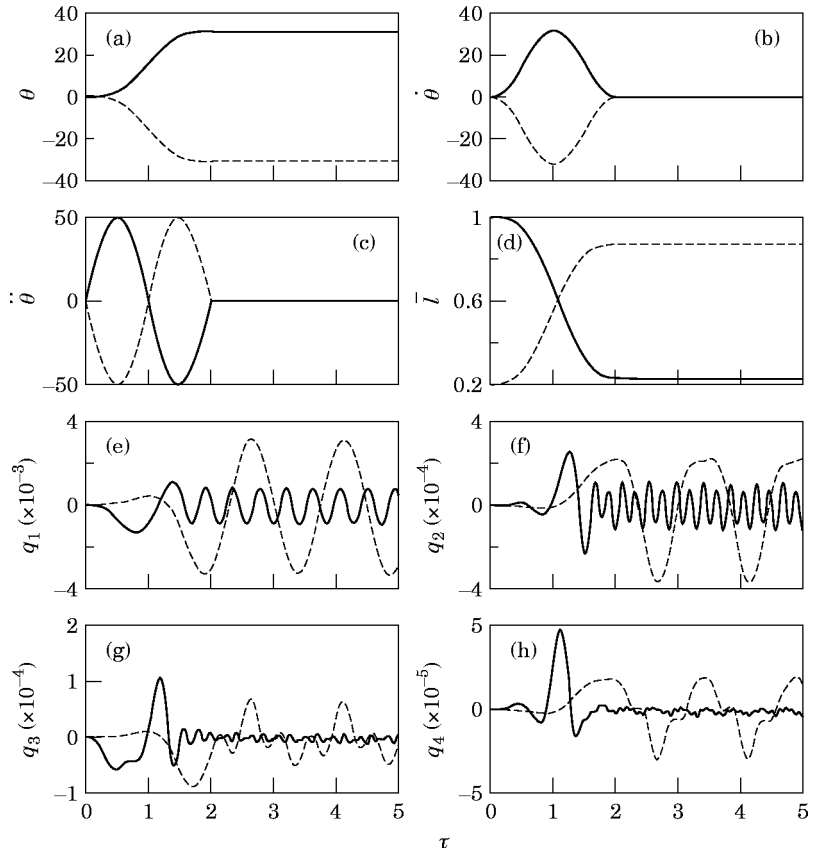

Figure 6. Motion-induced vibration with a desired cycloidal function during extraction and retraction. (a) desired angular position, (b) desired angular velocity, (c) desired angular acceleration, (d) length of the string, (e) vibration amplitudes of mode 1, (f) vibration amplitudes of mode 2, (g) vibration amplitudes of mode 3, (h) vibration amplitudes of mode 4. Key as for Figure 5.

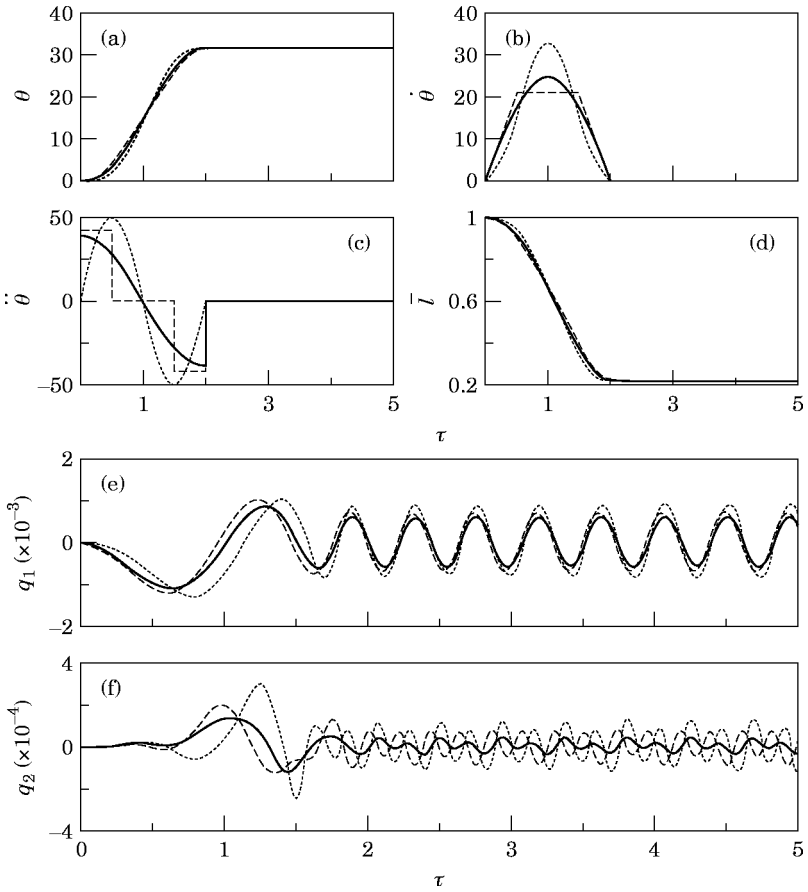

Figure 7. Motion-induced vibration in comparison with three kinds of the string motion for cases 1, 2 and 3. (a) desired angular position, (b) desired angular velocity, (c) desired angular acceleration, (d) length of the string, (e) vibration amplitudes of mode 1, (f) vibration amplitudes of mode 2. (——, simple harmonic; – – – –, trapezoidal; · · · · , cycloidal.)

In simulations, the reaching law for the VSC scheme is chosen as the controller of the elevator system to suppress these motion-induced vibrations. Various parameters of the system are the same as those in section 5.1. Furthermore, the first four modes ($N = 4$) in the Galerkin discretization are used for analysis. Thus, the sliding surface S is determined as

$$S = c_1 e_1 + c_2 e_2 + c_3 e_3 + c_4 e_4 + c_5 e_5 + c_6 e_6 + c_7 e_7 + c_8 e_8 + c_9 e_9 + c_{10} e_{10}. \tag{40}$$

And the VSC input is obtained as

$$\begin{aligned} u = (1/\Delta)[&-PS - Q|S|^{\kappa} S/(|S| + \delta) - c_1 e_6 - c_2 e_7 - c_3 e_8 - c_4 e_9 - c_5 e_{10} \\ &- c_6(L_{61} x_1 + L_{62} x_2 + L_{63} x_3 + L_{64} x_4 + n_6) - c_7(L_{71} x_1 + L_{72} x_2 + L_{73} x_3 + L_{74} x_4 + n_7) \\ &- c_8(L_{81} x_1 + L_{82} x_2 + L_{83} x_3 + L_{84} x_4 + n_8) - c_9(L_{91} x_1 + L_{92} x_2 + L_{93} x_3 + L_{94} x_4 + n_9) \\ &- (L_{10,1} x_1 + L_{10,2} x_2 + L_{10,3} x_3 + L_{10,4} x_4 + n_{10} - \ddot{\theta}_d)], \end{aligned} \tag{41}$$

where

$$\Delta = c_6 J_6 + c_7 J_7 + c_8 J_8 + c_9 J_9 + J_{10}.$$

The switching function described in equation (40) includes not only the tracking error of the rigid body motion but also the errors of the oscillation modes. The control input in VSC law is designed to ensure the situation that there are no tracking errors and transverse vibrations when the elevator system reaches the sliding condition $S = 0$ by the choice of the dynamics of switching function in equation (31). The boundary layer $\delta = 0{\cdot}0001$ is chosen. In the following simulations, the values of P, Q and the gains in matrix $\mathbf{C}$ are determined by the method of trial-and-error. In fact, many possible combinations of the constants and gains have been tried and we sift out the present combination which results in an optimum performance of tracking and stability. The numerical results of the control responses are divided into two parts: extrusion and retraction.

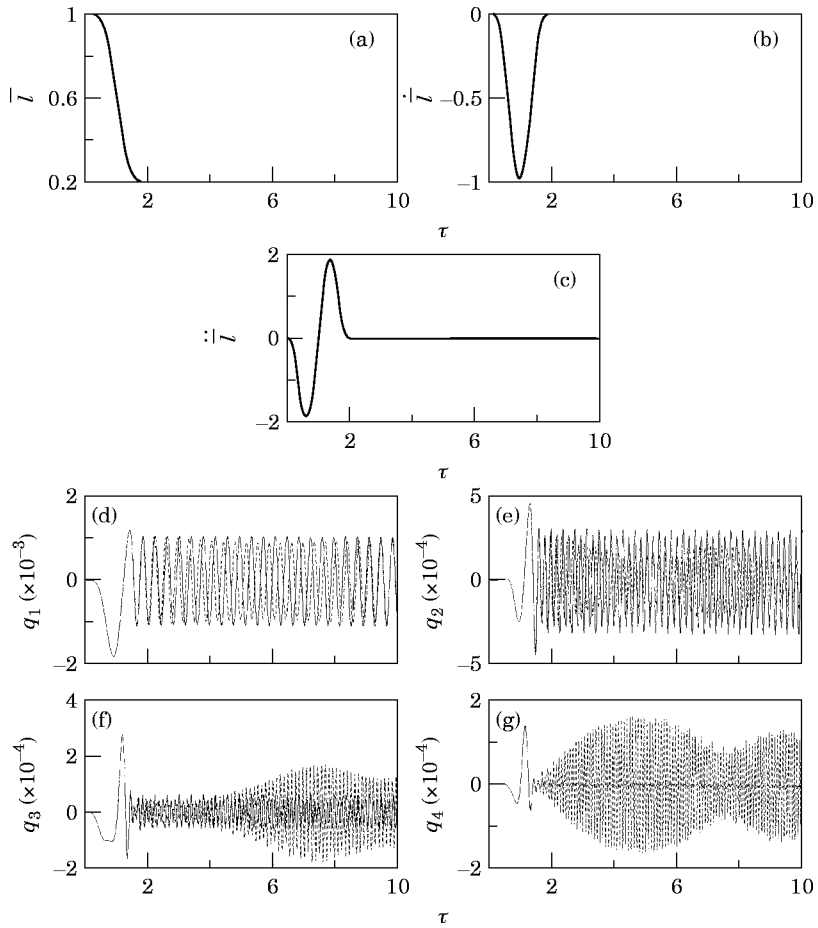

Figure 8. The non-linear effect on the transverse vibration of the string during retraction. (a) length of the string, (b) retraction velocity, (c) retraction acceleration, (d) vibration amplitudes of mode 1, (e) vibration amplitudes of mode 2, (f) vibration amplitudes of mode 3, (g) vibration amplitudes of mode 4. (——, linear; – – – –, non-linear.)

5.2.1. *Extrusion motion*

First, the vibration reduction of the elevator string during extrusion is discussed. During extrusion, the dominant vibration of the string takes place when the motion of the system is complete. The controller of VSC theory is designed to reduce the residual vibrations. Three desired trajectories are assumed as the same as those in section 5.1. A proper choice of the gain matrix and constants P and Q and will ensure the elevator system stable.

Case 1: cycloidal function. The gain matrix for the switching function which ensures that the system tends to maintain stability is given as follows:

$$\mathbf{C} = [-170 \quad 5 \quad 5{\cdot}5 \quad 3{\cdot}5 \quad 1{\cdot}5 \quad 150 \quad 1{\cdot}6 \quad 1{\cdot}5 \quad 0{\cdot}5 \quad 1],$$

and then the constant coefficients are chosen as $P = 10$ and $Q = 1$. The transient vibration responses, the time histories of angular position θ of the rotor and the length of string $\bar{l}$ versus the dimensionless time τ are illustrated in Figures 9(a–g). The solid lines in Figures 9(a) and 9(b) represent the tracking performances of θ and $\bar{l}$. The dash lines denote the desired behavior of the angular position of the rotor and the length of the string. The tracking performances of θ and $\bar{l}$ reach the desired position at $\tau = 30$.

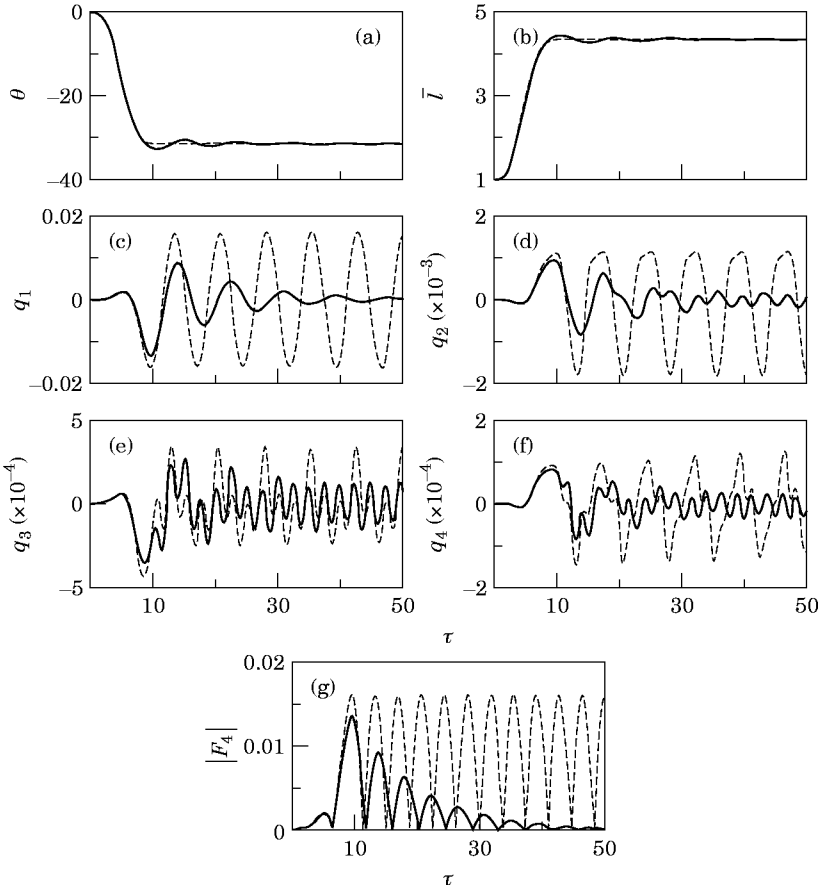

Figure 9. Motion-induced vibration suppression responses for the elevator system with a desired cycoidal function during extrusion. (a) angular position of rotor θ, (b) length of the string $\bar{l}$, (c) vibration amplitude of mode 1, (d) vibration amplitude of mode 2, (e) vibration amplitude of mode 3, (f) vibration amplitude of mode 4, (g) the norm of generalized co-ordinates. Key: ——, controlled system; – – – –, uncontrolled system.

Figures 9(c–f) show the transverse vibrations in comparison with the controlled system (solid line) and uncontrolled one (dash line) for the first four modes. It is observed that the transient amplitudes can be reduced by VSC law and the residual vibrations are clearly suppressed for all the modes. In Figure 9(g), the norms of the first four generalized co-ordinates for the controlled system (solid line) and uncontrolled one (dash line) are compared. The norm is evaluated by using equation (34). It is shown that the norm decays rapidly while the dimensionless time increases in the controlled system. The VSC theory ensures the system is stable because of the reduction of the vibration energy in the elevator string.

Case 2: trapezoidal function. For the trapezoidal desired trajectory, a suitable gain matrix for the switching function which makes the system stable is chosen as

$$\mathbf{C} = [-200 \quad 0{\cdot}45 \quad 0{\cdot}55 \quad 0{\cdot}36 \quad 2 \quad 150 \quad 1{\cdot}6 \quad 1{\cdot}5 \quad 0{\cdot}5 \quad 1],$$

and $P = 12$ and $Q = 1$. Figure 10(a) compares the norm of the first four generalized co-ordinates by using the VSC law (solid line) with that of the uncontrolled system (dash line). It is obvious that the norm of the controlled system is much smaller than that of the uncontrolled system. The transient and residual vibration amplitudes of the moving string are suppressed and the controller makes the system stable. This result is similar to case 1.

Case 3: simple harmonic function. In this case, simple harmonic motion is chosen to be the desired trajectory of the rotor. One selects the gain matrix and the constants for the sliding surface. They are

$$\mathbf{C} = [-210 \quad 0{\cdot}9 \quad 1{\cdot}2 \quad 0{\cdot}4 \quad 1{\cdot}5 \quad 160 \quad 1{\cdot}6 \quad 1{\cdot}5 \quad 0{\cdot}5 \quad 1],$$

and $P = 9$ and $Q = 1$. In Figure 10(b), the norm of the moving string in the controlled (solid line) and uncontrolled (dash line) system is plotted. As with previous discussions in cases 1 and 2, the VSC controller reduces the transverse amplitudes of the vibrating string and the total energy tends to decay. In these three cases, the major suppression effort appears in the residual vibrations. One concludes that the convergence of the tracking performance and the vibration reduction can be achieved concurrently during extrusion by the use of VSC.

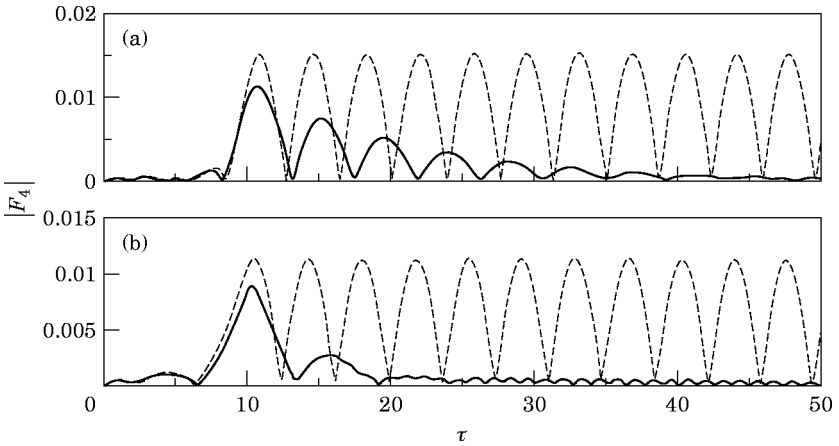

Figure 10. The norm of generalized co-ordinates of the elevator system during extrusion. (a) desired trapezoidal function, (b) desired simple harmonic function. Key as for Figure 9.

5.2.2. *Retraction motion*

The numerical results for the suppression control of the string during the retraction of the string are presented in this subsection. The desired motions of the rotor and the initial string length are selected as in section 5.1.

Case 1: trapezoidal function. For the desired trapezoidal trajectory, the gain matrix for the sliding function is chosen to be

$$\mathbf{C} = [-10000 \quad 4{\cdot}5 \quad 5 \quad 3{\cdot}6 \quad 10 \quad 3000 \quad 480 \quad 360 \quad 300 \quad 1].$$

The constant coefficients are chosen to be $P = 10$ and $Q = 1$. The time histories of the rotor angular position θ and the length of the string $\bar{l}$ are shown in Figures 11(a–b). The tracking performances of θ and $\bar{l}$ reach the desired position during retraction. The controlled and uncontrolled transient amplitudes of the first two modes only are illustrated in Figures 11(c–d). The motion-induced vibration during retraction is discussed in section 5.1. The major vibration amplitudes of the first two modes occur in the interval from $\tau = 0$ to $\tau = 2$. It is desired that the controller is designed to suppress the dominant transient vibrations. From these figures, it is observed that the transient amplitudes of vibration for the first two modes are apparently suppressed and the major quantities of residual vibrations are eliminated by using the controller (solid line). Figure 11(e) compares the controlled results (solid line) of the norms of the first four modes in the elevator string with the uncontrolled system (dash line). It is shown that the norm decreases quickly and converges asymptotically with time.

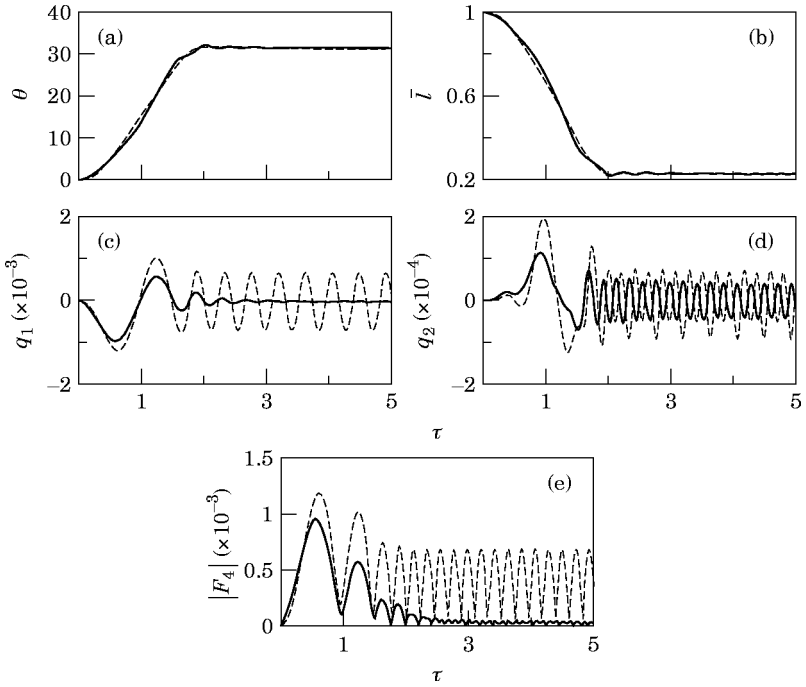

Figure 11. Motion-induced vibration suppression responses for the elevator system with a desired trapezoidal function during retraction. (a) angular position of rotor θ, (b) length of the string $\bar{l}$, (c) vibration amplitude of mode 1, (d) vibration amplitude of mode 2, (e) the norm of generalized co-ordinates. Key as for Figure 9.

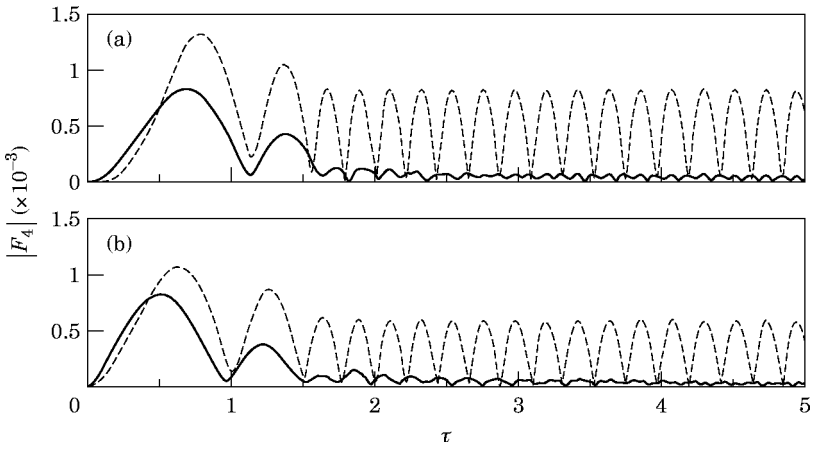

Figure 12. The norm of generalized co-ordinates of the elevator system during retraction. (a) desired cycoidal function, (b) desired simple harmonic function. Key as for Figure 9.

Case 2: cycloidal function. In this case, the desired cycloidal trajectory is used. The values of the gain matrix and the constants for the controlled system are chosen to be

$$\mathbf{C} = [-10000 \quad 8500 \quad 6500 \quad 3600 \quad 1{\cdot}5 \quad 3200 \quad 480 \quad 400 \quad 500 \quad 1],$$

and $P = 10$ and $Q = 10$. Figure 12(a) shows the norm of the first four modes of the elevator string in comparison with the controlled and the uncontrolled systems. It is observed that the norm in transient response is greatly suppressed and the residual vibration energy is reduced to a quite small value. It is due to the elimination of the most transverse amplitudes for the first two modes by using the VSC controller. The residual amplitude of mode 1 almost approaches zero. The results are the same as those discussed in case 1.

Case 3: simple harmonic function. In this case, one selects the value of gain matrix and the constants for the controlled system by using the desired simple harmonic trajectory. They are

$$\mathbf{C} = [-5000 \quad 550 \quad 450 \quad 1000 \quad 1{\cdot}5 \quad 2000 \quad 450 \quad 330 \quad 500 \quad 1],$$

and $P = 10$ and $Q = 1$. The numerical results of the norm with and without the VSC controller are compared in Figure 12(b). From this figure, one obtains a good convergence of the norm of the controlled system (solid line). As with the previous two cases, the norm in the controlled system is considerably smaller than that in the uncontrolled one.

6. CONCLUSIONS

A complete dynamic model for an elevator system that includes transverse string vibration and the rotor rotation has been formulated. In this paper, the dynamics of the PM synchronous servo motor, the time-dependent mass and radius of the rotor, and the time-dependent length of the string have been considered. First, the partial differential equations are derived by Hamilton's principle. Second, the dimensionless parameters and the Galerkin method are used to obtain the resulting ordinary differential equations. In numerical analysis, the convergence of the transient response problem in the Galerkin discretization and motion-induced vibration is studied.

The variable structure control has been developed for the vibration reduction of the elevator system. The controlled system is assigned simultaneously to meet the reaching condition and to make the elevator system asymptotically stable. Moreover, the advantage of this control method is straightforward and easy to implement. Finally, the numerical results obtained for some specific motions of rotor are given. From the numerical results, the following conclusions can be drawn:

1. In the Galerkin discretization, a finite number of modes is sufficient to represent the elastic vibration of the string in practice.
2. The variation of the rotor radius excites the transverse vibration of the moving string and the radius of the rotor is determined by the rotary motion of the rotor.
3. In the motion-induced vibrations, the transient amplitudes decrease during retraction and increase during extraction. The frequencies of oscillation increase during retraction and decrease during extrusion.
4. In considering the non-linear term, the frequency of the string vibration is quicker than that of the linear system. A beating phenomenon occurs after the rotor motion stops when the non-linear term is considered.
5. Due to the motion of the rotor and the transverse vibrations of the moving elevator string being coupled, it provides the opportunity that the transverse vibration of the string can be suppressed by controlling the current of the PM synchronous servo motor.
6. During extrusion, the residual vibrations are suppressed and the total energy of the elevator string decays fast by application of VSC theory. In addition, the transient amplitudes of the elevator string are reduced and the residual vibrations are almost eliminated during retraction. The vibration energy can be minimized and the elevator system is stabilized.

ACKNOWLEDGMENT

The authors are greatly indebted to the National Science Council of the R.O.C. for the support of the research through contract No. NSC 84-2212-E-033-012 .

REFERENCES

1. T. Yamamoto, K. Yasuda and M. Kato 1978 *Transactions of The Japan Society of Mechanical Engineers* **44-380c**, 17–24. Variation of a string with time variable length.
2. Y. Terumochi, M. Yoshizaw, I. Okazaki and Y. Tsujioka 1992 *Transactions of The Japan Society of Mechanical Engineers* **58-545c**, 17–24. Lateral oscillation of a moving elevator rope.
3. T. Kotera and R. Kawai 1988 *Nippon Kikai Gakksi Ronbunshu C Hen* **54**, 9–15. Vibrations of string with time-varying length (2nd Report, Free vibrations induced by initial displacements).
4. F. Fung, and W. H. Cheng 1993 *Journal of the Chinese Society of Mechanical Engineers* **12**, 229–239. Free vibration of a string/slider nonlinear coupling system.
5. L. Cventianin 1984 *Journal of Sound and Vibration* **97**, 181–187. Vibrations of a textile machine rotor.
6. L. Cventianin 1986 *Mechanism and Machine Theory* **21**, 29–32. The vibrations of a textile machine rotor with nonlinear characteristics.
7. A. P. Bessonov 1974 *Osnovji sinamiki mechanizmoves peremennojzvan zvenjev*. Moskva: Nausa.
8. M. Vance and J. Lee 1974 *Transactions of the American Society of Mechanical Engineers*, *Journal of Engineering for Industry* 660–668. Stability of high speed rotors with internal friction.
9. B. K. Bose 1988 *Institute of Electrical and Electronics Engineers*, *Transactions on Industrial Electronics* **35**, 160–176. Technology trends in microcomputer control of electrical machines.
10. P. C. Sen 1990 *Institute of Electrical and Electronics Engineers*, *Transactions on Industrial Electronics* **37**, 562–575. Electric motor drives and control-past, present, and future.

11. R. STRUNCE and R. W. CARMAN 1984 *American Institute of Aeronautics and Astronautics Journal* **84**, 348–356. Active control of space structures: a status report.
12. S. S. RAO, T. S. PAN and V. B. VENKAYYA 1990 *Applied Mechanics Review* **43**, 99–117. Modeling, control, and design of flexible structures: a survey.
13. C. J. RADCLIFF and C. D. MOTE, JR. 1983 *Transactions of the American Society of Mechanical Engineers*, *Journal of Dynamic Systems*, *Measurement and Control* **105**, 39–45. Identification and control of rotating disk vibration.
14. C. D. MOTE, JR. and S. HOLOYEN 1978 *Transactions of the American Society of Mechanical Engineers*, *Journal of Engineering for Industry* **100**, 119–126. Feedback control of sawblade temperature with induction heating.
15. M. J. BALAS 1982 *Institute of Electrical and Electronics Engineers*, *Automatic Control* **27**, 15–33. Trends in large space structure control theory: fondest hopes, widest dreams.
16. S. G. TZAFESTAS and P. STAVROULAKIS 1983 *Journal of The Franklin Institute* **315**, 285–305. Recent advance in the distributed parameter systems.
17. A. G. ULSOY 1984 *Transactions of the American Society of Mechanical Engineers*, *Journal of Dynamic Systems*, *Measurement and Control* **106**, 6–14. Vibration control in rotating or translating elastic systems.
18. B. YANG and C. D. MOTE, JR. 1991 *Transactions of the American Society of Mechanical Engineers*, *Journal of Applied Mechanics* **58**, 189–196. Active vibration control of the axially moving string in the *s* domain.
19. V. I. UTKIN 1978 *Sliding Modes and Their Application in Variable Structure Systems*. Mir, Moscow.
20. U. ITKIS 1976 *Control Systems of Variable Structure*. New York: Wiley.
21. B. A. WHITE and P. M. SILSON 1984 *Institute of Electrical Engineers Proceedings* **131**, 85–91. Reachability in variable structure control systems.
22. J. Y. HUNG, W. GAO and J. C. HUNG 1993 *Institute of Electrical and Electronics Engineers*, *Transactions of Industrial Electronics* **40**, 1–22. Variable structure control: a survey.
23. A. FICOLA, M. L. CAVA and P. MURACA 1992 *International Federation of Automatic Control*, *Motion Control for Intelligent Automation*, *Perugia*, *Italy*, 27–29. A simplified strategy to implement sliding mode control of a two-joints robot with a flexible forearm.
24. R. F. FUNG and C. C. LIAO 1995 *International Journal of Mechanics Science* **37**, 985–993. Application of variable structure control in the nonlinear string system.
25. C. L. TSAI 1996 *Master Thesis*, *Chun Yuan Christian University*, *Taiwan*. Dynamic analysis of a nonlinear coupled textile/rotor system.
26. W. J. WANG and J. L. LEE 1993 *Journal of Control System and Technology* **1**, 19–25. Hitting time reduction and chattering attenuation in variable structure systems.

APPENDIX A

A1. VIBRATION OF STRING

From Figure 1, the position and velocity vectors of any point on the string after deformation are respectively

$$\mathbf{r} = x(t)\mathbf{i} + [R(t) + w(x, t)]\mathbf{j}, \qquad \mathbf{V} = \mathrm{d}\mathbf{r}/\mathrm{d}t = \dot{x}\mathbf{i} + (\dot{R}(t) + w_t + \dot{x}w_x)\mathbf{j}, \quad \text{(A1, A2)}$$

where **i**, **j** are unit vectors that point in the directions of increasing x and y, respectively.

The Lagrangian function for the string is the kinetic energy minus the potential energy. Thus, one has

$$L_s = \frac{1}{2}\int_0^{l(t)} \rho \mathbf{V}\cdot\mathbf{V}\,\mathrm{d}x - \int_0^{l(t)} (T\varepsilon_E + \tfrac{1}{2}EA\varepsilon_E^2)\,\mathrm{d}x$$

$$= \frac{1}{2}\int_0^{l(t)} \{\rho(\dot{x}^2 + w_t^2 + \dot{x}^2 w_x^2 + \dot{R}^2(t) + 2\dot{x}w_x w_t + 2\dot{x}w_x\dot{R}(t) + 2\dot{R}(t)w_t)$$

$$- [T(x, l(t))w_x^2 + \tfrac{1}{4}EAw_x^4]\}\,\mathrm{d}x = \int_0^{l(t)} L_s^*(x(t), t; w, w_x, w_t)\,\mathrm{d}x, \qquad \text{(A3)}$$

where $\varepsilon_E = \frac{1}{2}w_x^2$ is the engineering strain, EA denotes the rigidity of the string, $T\varepsilon_E$ and $\frac{1}{2}EA\varepsilon_E^2$ are respectively the strain energies due to the initial tension and the deflection. The latter is measured from the initially tensioned configuration. Since the string is hung under not only the weight of the concentrated mass at the lower end but also its own weight, the tension can be expressed as

$$T(x, l(t)) = Mg + \rho g(l(t) - x). \tag{A4}$$

A2. ROTATING ROTOR

The Lagrangian function of the rotor is

$$L_r = \tfrac{1}{2}I(t)\dot{\theta}^2. \tag{A5}$$

In order to derive the virtual work done by the initial tension T on the rotor, the virtual displacement at the connection point will be obtained first. The string length can be written as

$$l(t) = l_0 - \int_0^{\theta} R(\varepsilon)\,\mathrm{d}\varepsilon = l_0 - (2/3K)[(R_0^2 + K\theta(t))^{3/2} - R_0^3], \tag{A6}$$

where

$$K = R_1 h/\pi.$$

The virtual displacement of the connection point is

$$\delta l(t) = -(R_0^2 + K\theta(t))^{1/2}\,\delta\theta = -R(t)\,\delta\theta. \tag{A7}$$

The virtual work done by the external torque and the initial tension can be expressed as

$$\delta W = \tau_e\,\delta\theta + T \cdot \delta l(t) = \{\tau_e - T(0, l(t))R(t)\}\,\delta\theta. \tag{A8}$$

A3. FORMULATION FOR THE COUPLED ELEVATOR SYSTEM

To obtain the equations for the coupled system, the calculus of variations and Hamilton's principle are applied. However, the application of the principle is not straightforward, since there is a moving boundary involved at $x = l(t)$, where the position is not specified.

The entire system including the textile with length $0 \leqslant x \leqslant l(t)$ and the rotor is considered. Hamilton's principle can be written as

$$\int_{t_1}^{t_2}\left[\delta\int_0^{l(t)} L_s^*(x, t; w, w_x, w_t)\,\mathrm{d}x + \delta L_r(t; \dot{\theta}) + \delta W\right]\mathrm{d}t = 0, \tag{A9}$$

where t_1 and t_2 are two arbitrary end times. Taking the variation in equation (A9), applying

the partial integration technique, using Leibnitz's rule, and collecting like terms, one obtains

$$0 = \int_{t_1}^{t_2} \left\{ L_s^*(l(t), t; w(l(t), t))\, \delta l(t) + \int_0^{l(t)} \delta L_s^*(x(t), t; w, w_x, w_t)\, \mathrm{d}x + \delta L_r(t; \dot{\theta}) + \delta W \right\} \mathrm{d}t$$

$$= \int_{t_1}^{t_2} \left\{ -R(t) L_s^*(l(t), t; w(l(t), t))\delta\theta + \int_0^{l(t)} \left(\frac{\partial L_s^*}{\partial w} - \frac{\partial}{\partial x}\frac{\partial L_s^*}{\partial w_x} - \frac{\partial}{\partial t}\frac{\partial L_s^*}{\partial w_t} \right) \delta w\, \mathrm{d}x \right.$$

$$\left. + \left[\frac{\partial L_s^*}{\partial w_x}\delta w \right]_{x=0}^{x=l(t)} + \left(\frac{\partial L_r}{\partial \theta} - \frac{\partial}{\partial t}\frac{\partial L_r}{\partial \dot{\theta}} \right) \delta\theta + [\tau_e - T(0, l(t))R(t)]\, \delta\theta \right\} \mathrm{d}t$$

$$+ \left[\int_0^{l(t)} \frac{\partial L_s^*}{\partial w_i}\delta w\, \mathrm{d}x + \frac{\partial L_r}{\partial \dot{\theta}}\delta\theta \right]_{t_1}^{t_2}. \tag{A10}$$

The varied path coincides with the true path at the two end points t_1 and t_2. It follows that $\delta w(t_1) = \delta w(t_2) = 0$ and $\delta\theta(t_1) = \delta\theta(t_2) = 0$. From equation (A10) we can obtain Lagrange's equations for the string and rotor, respectively, as

$$\partial L_s^*/\partial w - (\partial/\partial x)(\partial L_s^*/\partial w_x) - (\partial/\partial t)(\partial L_s^*/\partial w_t) = 0, \qquad 0 < x < l(t), \tag{A11}$$

$$\partial L_r/\partial\theta - (\partial/\partial t)(\partial L_r/\partial\dot{\theta}) + \tau_e - R(t)[T(0, l(t)) + L_s^*(l(t), t; w(l(t), t))] = 0, \tag{A12}$$

and the boundary conditions are

$$w(0, t) = 0, \qquad w(l(t), t) = 0. \tag{A13, A14}$$

Substituting the Lagrangian functions (A2) and (A3) of the string and rotor into equations (A11) and (A12), one obtains the governing equations (4a) and (4b).

APPENDIX B

The elements of the symmetric inertia matrix **M** are given as

$$\mathbf{M}(m, n) = \begin{cases} 1, & \text{if } m = n \\ 0, & \text{if } m \neq n \end{cases}, \qquad (m, n = 1, \ldots, N), \tag{B1}$$

$$\mathbf{M}(m, N+1) = \frac{\alpha}{2\bar{R}} Z_m - \sum_{n=1}^{N} \bar{R} B_{mn}, \qquad \mathbf{M}(N+1, n) = 0, \tag{B2, B3}$$

$$\mathbf{M}(N+1, N+1) = \frac{\Lambda_M + r^2\bar{I}}{r}, \tag{B4}$$

where

$$\alpha = R_1 h/l_0^2\pi, \qquad Z_m = (\sqrt{2\bar{l}}/m\pi)[1 - (-1)^m].$$

The elements of the vector **H** are

$$\mathbf{H}(m) = \sum_{n=1}^{N} [(2A_{mn} + 2\bar{R}\dot{\theta}B_{mn})\dot{q}_n] + \sum_{n=1}^{N} [(-\bar{R}_\tau\dot{\theta}^2B_{mn} - 2\bar{R}\dot{\theta}E_{mn} + \bar{R}^2\dot{\theta}^2F_{mn})q_n],$$

$$m, n = 1, \ldots, N, \tag{B5}$$

$$\mathbf{H}(N+1) = (\bar{B}_M + r^2\bar{I})/r + (r\bar{R}/2)[\bar{R}^2\dot{\theta}^2 + 2\bar{g}(\bar{M} + \bar{l})] + \sum_{n=1}^{N} S_M b_n^r q_n$$

$$+ \sum_{n=1}^{N}\sum_{i=1}^{N} S_M c_{ni}^r q_n q_i + \sum_{n=1}^{N}\sum_{i=1}^{N}\sum_{j=1}^{N}\sum_{k=1}^{N} S_M d_{nijk}^r q_n q_i q_j q_k, \tag{B6}$$

where

$$S_M = (\Lambda_M + r^2\bar{I})/r.$$

The elements of the symmetric stiffness matrix **K** are

$$\mathbf{K}(m, n) = D_{mn} + \bar{g}B_{mn} - (1 + \bar{l}/\bar{M})F_{mn} + (1/\bar{M})H_{mn}, \qquad m, n = 1, \ldots, N, \tag{B7}$$

$$\mathbf{K}(m, N+1) = 0, \qquad \mathbf{K}(N+1, n) = 0, \tag{B8}$$

and the elements of the vector **U** are

$$\mathbf{U}(m) = 0, \qquad \mathbf{U}(N+1) = \bar{A}_Q, \qquad m = 1, \ldots, N. \tag{B9}$$

APPENDIX C

The time-varying coefficients of equations (25a) and (25b):

$$a_{mn}(\bar{l}, \dot{\bar{l}}) = 2A_{mn}(\bar{l}, \dot{\bar{l}}) + 2\xi_\tau B_{mn}(\bar{l}),$$

$$b_{mn}(\bar{l}, \dot{\bar{l}}, \ddot{\bar{l}}) = (\xi_{\tau\tau} + \bar{g})B_{mn}(\bar{l}) + D_{mn}(\bar{l}, \dot{\bar{l}}, \ddot{\bar{l}}) + 2\xi_\tau E_{mn}(\bar{l}, \dot{\bar{l}})$$

$$+ (\xi_\tau^2 - 1 - (1/\bar{M})\bar{l})F_{mn}(\bar{l}) + (1/\bar{M})H_{mn},$$

$$c_{mijk}(\bar{l}) = \tfrac{3}{2}\beta^2 N_{mijk}(\bar{l}), \qquad G_m = -\bar{R}_{\tau\tau}(\sqrt{2\bar{l}}/m\pi)[1 - (-1)^m],$$

$$a^r = (\bar{B}_M + r^2 I_\tau)/(\Lambda_M + r^2\bar{I}), \qquad b_n^r(\bar{l}) = \frac{r^2\xi_\tau\bar{R}\bar{R}_\tau}{\Lambda_M + r^2\bar{I}}\frac{n\pi}{\sqrt{\bar{l}^3}}(-1)^n,$$

$$c_{ni}^r(\bar{l}) = (\xi_\tau^2 - \bar{M}\bar{g})\frac{r^2\bar{R}}{(\Lambda_M + r^2\bar{I})}\frac{ni\pi^2}{\bar{l}^3}(-1)^{(n+i)},$$

$$d_{nijk}^r(\bar{l}) = [r^2\beta^2\bar{R}/(8(\Lambda_M + r^2\bar{I}))]\ (nijk\pi^4/\bar{l}^6)(-1)^{(n+i+j+k)},$$

$$F^r(\bar{l}) = r\bar{A}_Q/(\Lambda_M + r^2\bar{I}) - r^2\bar{R}/(2(\Lambda_M + r^2\bar{I}))[\xi_\tau^2 + \bar{R}_\tau^2 + 2\bar{g}(\bar{M} + \bar{l})]$$

where

$$A_{mn}(\bar{l}, \dot{\bar{l}}) = \int_0^l \dot{\varphi}_n \varphi_m \, \mathrm{d}\xi, \qquad B_{mn}(\bar{l}) = \int_0^l \varphi_n' \varphi_m \, \mathrm{d}\xi, \qquad C_{mn}(\bar{l}) = \xi_{\tau\tau} \int_0^l \varphi_n' \varphi_m \, \mathrm{d}\xi,$$

$$D_{mn}(\bar{l}, \dot{\bar{l}}, \ddot{\bar{l}}) = \int_0^l \ddot{\varphi}_n \varphi_m \, \mathrm{d}\xi, \qquad E_{mn}(\bar{l}, \dot{\bar{l}}) = \int_0^l \dot{\varphi}_n' \varphi_m \, \mathrm{d}\xi, \qquad F_{mn}(\bar{l}) = \int_0^l \varphi_n'' \varphi_m \, \mathrm{d}\xi,$$

$$N_{mijk}(\bar{l}, \dot{\bar{l}}, \ddot{\bar{l}}) = \int_0^l \varphi_i' \varphi_j' \varphi_k'' \varphi_m \, \mathrm{d}\xi, \qquad H_{mn}(\bar{l}) = \int_0^l \xi \varphi_n \varphi_m \, \mathrm{d}\xi.$$